Dyes and Pigments 194 (2021) 109615

Contents lists available at ScienceDirect

Dyes and Pigments

journal homepage: www.elsevier.com/locate/dyepig

Electropolymerization of V-shape D-A-D type monomers for efficient and tunable electrochromics

Wenyuan Wang [a], Hongjin Chen [a], Youfeng Yue [b], Rui Zhang [a,c], Jian Liu [a,c,*]

[a] College of Chemical Engineering, Jiangsu Key Lab of Biomass-based Green Fuels and Chemicals, Nanjing Forestry University, Nanjing, 210037, China
[b] Research Institute for Advanced Electronics and Photonics, National Institute of Advanced Industrial Science and Technology (AIST), 1-1-1 Higashi 305-8565, Tsukuba, Japan
[c] Jiangsu Co-Innovation Center of Efficient Processing and Utilization of Forest Resources, Nanjing Forestry University, Nanjing, 210037, China

ARTICLE INFO

Keywords:
Electrochromic
Donor-acceptor-donor
V-shape
Quinoxaline

ABSTRACT

Five novel donor-acceptor-donor (D-A-D) type monomers (**VQ1** ~ **VQ5**) with a common V-shape configuration have been developed and further electropolymerized for electrochromic applications. The monomers were designed by introducing two triphenylamine groups into the 2- and 3- position of the quinoxaline derivates, respectively. These redox-active monomers could be electrodeposited robustly on the ITO electrodes in an electrolyte solution *via* the oxidative coupling reactions between triphenylamine radical cations. The obtained thin polymer films (**PVQ1** ~ **PVQ5**) exhibited reversible redox behaviours and obvious color changes upon voltage variation. All these polymers exhibited excellent electrochromic performances involving high optical contrast (over 70%), short response time (less than 2 s) and high coloration efficiency (over 200 cm^2 C^{-1}). Moreover, the optical properties of these polymers in both neutral state and oxidation state can be tuned by variation of the additional substituents on the quinoxaline parts, respectively.

1. Introduction

Electrochromic devices that can change colors under an applied voltage, have received considerable attention due to their potential applications in many fields, such as optical displays, smart windows, antiglare rearview mirrors, and so on [1–4]. During the past decades, tremendous research efforts have been devoted to the development of efficient electrochromic materials which play a crucial role in electrochromic devices, with the aim of low cost, high optic contrast, long-term stability and customized color variation [5–13]. So far, various kinds of electrochromic materials involving metal oxides, viologens, conjugated conducting polymers, and metal coordination complexes have been reported [14–24].

Among them, organic electrochromic materials have been demonstrated to be possessing many advantages including short switching times, easy color-tuning, and high coloration efficiency [25]. Polyarylamine derivatives have been demonstrated as a kind of active electrochromic materials due to their unique reversible redox behaviour of the arylamine moieties, which can be colorized upon electro-oxidation process [26–30]. To improve the performance of polyarylamine-based electrochromic materials, a valid strategy in molecular engineering is to introduce an electron accepting moiety into the conjugated backbones [17]. The state-art linear D-A-D type configuration achieved the improvement of stability, switch speed and coloration efficiency [31]. However, the intrinsic strong intramolecular charge transfer transition in D-A-D type conjugated polymers lead to a broad and high absorption in visible region and reduce their light transmittance in their neutral states, which limited their practical application in smart window for energy saving-building [32–34]. On the other hand, the frequent use of noble metal catalysis for the coupling reaction between donor and acceptor parts during the synthesis of D-A-D type conjugated compounds also reduced their cost performance [35]. Although the cut of the conjugation can obtain colorless electrochromic materials, it would result in the boundedness for color tuning and the probable deterioration of device performance [29]. Therefore, the development of color tunable conjugated D-A-D type electrochromic materials among colorless and colorful is still a challenge [36–41].

Herein, we developed five novel D-A-D type monomers with a common V-shape configuration, in which two triphenylamine groups were introduced into the 2- and 3- position of the quinoxaline derivates,

* Corresponding author. College of Chemical Engineering, Jiangsu Key Lab of Biomass-based Green Fuels and Chemicals, Nanjing Forestry University, Nanjing, 210037, China.
E-mail address: liu.jian@njfu.edu.cn (J. Liu).

https://doi.org/10.1016/j.dyepig.2021.109615
Received 18 March 2021; Received in revised form 25 June 2021; Accepted 28 June 2021
Available online 29 June 2021

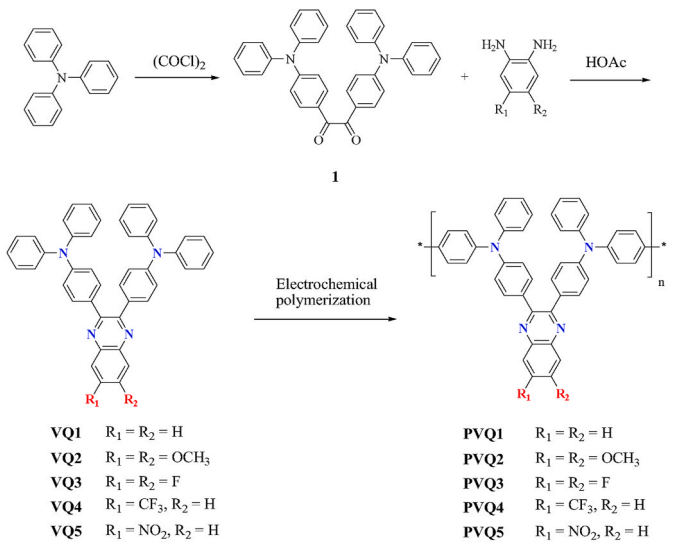

Scheme 1. Molecular structures and synthetic routes of V-shape monomers (**VQ1** ~ **VQ5**) and the corresponding D-A-D type electrochromic polymers (**PVQ1** ~ **PVQ5**).

respectively. The synthesis of V-shape monomers **VQ1** ~ **VQ5** can be easily achieved by condensation reactions between diketone and diamines, respectively. The corresponding D-A-D polymers **PVQ1** ~ **PVQ5** were successfully prepared by electropolymerization, which exhibited efficient electrochromic properties and device performances. Furthermore, the color of the present D-A-D type electrochromic polymers in both neutral and oxidation states can be easily tuned by introducing addition substitutes on the quinoxaline parts, which guaranteed their potential applications in smart windows.

2. Experimental

All chemicals and reagents were used as received from chemical companies without further purification. Column chromatography was performed using silica gel as a stationary phase. UV–Vis spectra were measured in dichloromethane (DCM) solution or thin film on ITO glass using LAMBDA 365 Spectrophotometer (PerkinElmer). Cyclic voltammetry (CV) was performed on a CHI 760E potentiostat/galvanostat system. Platinum electrode was used as a working electrode, Ag/AgCl in saturated KNO_3 (aq.) as a reference electrode, and a platinum wire as a counter electrode. The NMR measurements were performed by a DRX-400 spectrometer (Bruker BioSpin). Mass spectra were measured on a Shimadzu Biotech matrix-assisted laser desorption ionization (MALDI) mass spectrometer. TGA were characterized by TG 209F-1 (NETZSCH).

*Preparation of compound **1***. To a stirred solution of triphenylamine (15 g, 61.22 mmol) in anhydrous CH_2Cl_2 (100 mL) was added anhydrous aluminum chloride (8.17 g, 10.28 mmol) portion wise at 0 °C under N_2 atmosphere. Oxalyl chloride (3.95 g, 25.48 mmol) was added dropwise and maintained the rection system below 0 °C. The reaction mixture was stirred at room temperature for 12 h, and then treated with water (50 mL), extracted twice with CH_2Cl_2 (40 mL × 2). The combined organic layers were washed twice with water and once with brine, dried over anhydrous magnesium sulfate. After evaporation of the solvent under reduced pressure, The residue was treated with MeOH (15 mL), the solid was collected by filtration, and dried under vacuum to yield the desired product **2a** as a white powder (7.07 g, 51%). ^{1}H NMR (400 MHz, $CDCl_3$) δ: 7.80 (d, J = 9.0 Hz, 2H), 7.38–7.34 (m, 4H), 7.21–7.17 (m, 6H), 6.98 (d, J = 9.0 Hz, 2H). ^{13}C NMR (100 MHz, $CDCl_3$) δ: 193.36, 153.43, 145.96, 131.66, 129.75, 126.40, 125.28, 119.00. ESI (m/z): Calcd for $C_{38}H_{28}N_2O_2$, 544.22 $(M)^+$; found, 544.21.

*Preparation of monomer **VQ1***. To a stirred solution of compound **1** (163 mg, 0.3 mmol) in acetic acid (40 mL) was added benzene-1,2-diamine (33 mg, 0.3 mmol) at room temperature. The reaction mixture was stirred at 90 °C under N_2 atmosphere for 12 h. Evaporation of the acetic acid under reduced pressure and the residue was treated with water (50 mL), extracted twice with CH_2Cl_2 (50 mL × 2). The combined organic layers were washed twice with water and once with brine, dried over anhydrous magnesium sulfate. After removing the solvent under reduced pressure, the residue was purified by chromatography using hexane/EA (10/1, v/v) as an eluent to yield compound **3a** as an orange solid (130 mg, 71%). ^{1}H NMR (400 MHz, $CDCl_3$) δ: 8.13 (dd, J_1 = 6.4 Hz, J_2 = 3.4 Hz, 2H), 7.73 (dd, J_1 = 6.4 Hz, J_2 = 3.4 Hz, 2H), 7.44 (d, J = 8.8 Hz, 4H), 7.31–7.26 (m, 8H), 7.13 (d, J = 7.6 Hz, 8H), 7.08–7.03 (m, 8H). ^{13}C NMR (100 MHz, $CDCl_3$) δ: 160.15, 156.43, 155.82, 149.82, 149.11, 136.85, 130.46, 128.49, 123.75, 121.38, 118.24, 114.87. ESI (m/z): Calcd for $C_{44}H_{32}N_4$, 616.26 (M^+); found,

Table 1
Optical and redox parameters of monomers **VQ1** ~ **VQ5**[a].

Monomer	[a]λ_{max} (nm)	[b]$S^{+/0}$ (eV)	[c]S+/* (eV)	[d]$E_{0\text{-}0}$ (eV)
VQ1	401	0.93	−1.65	2.58
VQ2	399	0.91	−1.72	2.63
VQ3	410	0.95	−1.55	2.50
VQ4	420	0.96	−1.47	2.43
VQ5	460	0.97	−1.18	2.15

[a] The absorption spectra were measured in CH_2Cl_2 solution.
[b] The $S^+/0$ corresponding to the ground-state oxidation potential (*vs* NHE) in CH_2Cl_2 internally calibrated with ferrocene.
[c] $S^+/* = S^+/0 - E_{0\text{-}0}$, where $E_{0\text{-}0}$ is the zero-zero transition energy.
[d] $E_{0\text{-}0}$ values were estimated from the onset of the absorption spectra in CH_2Cl_2.

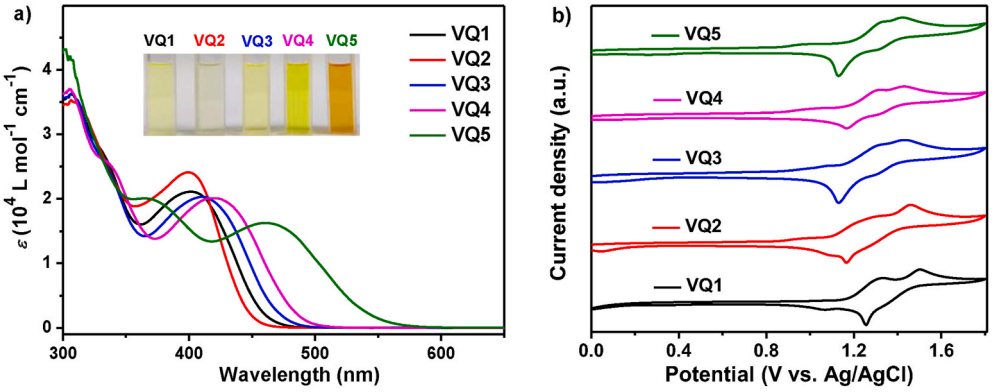

Fig. 1. a) Absorption spectra of V-shape D-A-D type monomers **VQ1** ~ **VQ5** in CH_2Cl_2; b) Cyclic voltammograms of monomers **VQ1** ~ **VQ5** in CH_2Cl_2/$TBAPF_6$ (0.1 M), [c] = 1 × 10^{-4} mol L^{-1}, 293 K, scan rate = 100 mV s^{-1}.

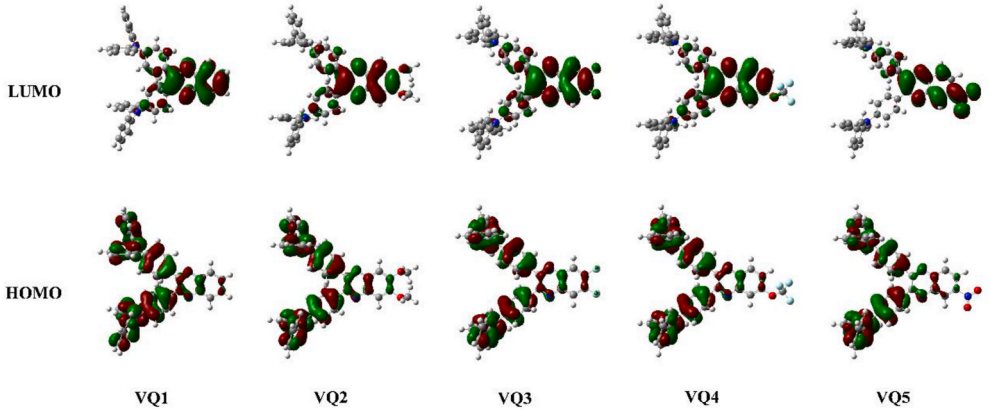

Fig. 2. The HOMO and LUMO of monomers **VQ1** ~ **VQ5** calculated at B3LYP/6-31G** level.

616.26.

*Preparation of monomer **VQ2***. To a stirred solution of compound **1** (163 mg, 0.3 mmol) in acetic acid (40 mL) was added 4,5-dimethoxybenzene-1,2-diamine (50 mg, 0.3 mmol) at room temperature. The reaction mixture was stirred at 90 °C under N_2 atmosphere for 12 h. Evaporation of the acetic acid under reduced pressure and the residue was treated with water (50 mL), extracted twice with CH_2Cl_2 (50 mL × 2). The combined organic layers were washed twice with water and once with brine, dried over anhydrous magnesium sulfate. After removing the solvent under reduced pressure, the residue was purified by chromatography using hexane/EA (10/1, v/v) as an eluent to yield compound **3a** as an orange solid (155 mg, 76%). ^{1}H NMR (400 MHz, $CDCl_3$) δ: 7.48–7.42 (m, 6H), 7.29 (t, J = 7.8 Hz, 8H), 7.15 (d, J = 7.6 Hz, 8H), 7.09–7.05 (m, 8H), 4.09 (s, 6H). ^{13}C NMR (100 MHz, $CDCl_3$) δ: 152.63, 150.75, 148.10, 147.44, 138.17, 133.14, 130.69, 129.33, 124.79, 123.27, 122.58, 106.70, 56.40. ESI (*m/z*): Calcd for $C_{46}H_{36}N_4O_2$, 676.28 (M^+); found, 676.28.

*Preparation of monomer **VQ3***. To a stirred solution of compound **1** (163 mg, 0.3 mmol) in acetic acid (40 mL) was added 4,5-difluorobenzene-1,2-diamine (43 mg, 0.3 mmol) at room temperature. The reaction mixture was stirred at 90 °C under N_2 atmosphere for 12 h. Evaporation of the acetic acid under reduced pressure and the residue was treated with water (50 mL), extracted twice with CH_2Cl_2 (50 mL × 2). The combined organic layers were washed twice with water and once with brine, dried over anhydrous magnesium sulfate. After removing the solvent under reduced pressure, the residue was purified by chromatography using hexane/EA (10/1, v/v) as an eluent to yield compound **3a** as an orange solid (143 mg, 73%). ^{1}H NMR (400 MHz, $CDCl_3$) δ: 7.87 (t, J = 9.2 Hz, 2H), 7.45 (d, J = 8.6 Hz, 4H), 7.30 (t, J = 7.8 Hz, 8H), 7.16 (d, J = 7.8 Hz, 8H), 7.09 (t, J = 7.2 Hz, 4H), 7.06 (d, J = 8.6 Hz, 4H). ^{13}C NMR (100 MHz, $CDCl_3$) δ: 153.39, 150.96, 150.83, 148.84, 147.22, 138.35, 138.29, 138.19, 131.78, 130.74, 129.45, 125.16, 123.68, 121.90, 114.71, 114.65, 114.59, 114.53. ESI (*m/z*): Calcd for $C_{46}H_{36}N_4O_2$, 652.24 (M^+); found, 652.24.

*Preparation of monomer **VQ4***. To a stirred solution of compound **1** (163 mg, 0.3 mmol) in acetic acid (40 mL) was added 4-(trifluoromethyl)benzene-1,2-diamine (53 mg, 0.3 mmol) at room temperature. The reaction mixture was stirred at 90 °C under N_2 atmosphere for 12 h. Evaporation of the acetic acid under reduced pressure and the residue was treated with water (50 mL), extracted twice with CH_2Cl_2 (50 mL × 2). The combined organic layers were washed twice with water and once with brine, dried over anhydrous magnesium sulfate. After removing the solvent under reduced pressure, the residue was purified by chromatography using hexane/EA (10/1, v/v) as an eluent to yield compound **3a** as an orange solid (142 mg, 69%). ^{1}H NMR (400 MHz, $CDCl_3$) δ: 8.43 (s, 1H), 8.22 (d, J = 8.8 Hz, 1H), 7.88 (dd, J_1 = 8.8 Hz, J_2 = 1.7 Hz, 1H), 7.47 (dd, J_1 = 8.8 Hz, J_2 = 7.0 Hz, 4H), 7.29 (t, J = 8.0 Hz, 8H), 7.15 (d, J = 8.2 Hz, 8H), 7.10 (d, J = 7.4 Hz, 4H), 7.04 (d, J = 8.5 Hz, 4H). ^{13}C NMR (100 MHz, $CDCl_3$) δ: 155.06, 154.51, 149.08, 149.01, 147.16, 142.10, 140.00, 131.60, 130.84, 130.76, 130.12, 129.44, 127.04, 125.21, 123.76, 121.77. ESI (*m/z*): Calcd for $C_{45}H_{31}F_3N_4$, 684.25 (M^+); found, 684.25.

*Preparation of monomer **VQ5***. To a stirred solution of compound **1** (163 mg, 0.3 mmol) in acetic acid (40 mL) was added 4-nitrobenzene-1,2-diamine (46 mg, 0.3 mmol) at room temperature. The reaction mixture was stirred at 90 °C under N_2 atmosphere for 12 h. Evaporation of the acetic acid under reduced pressure and the residue was treated with water (50 mL), extracted twice with CH_2Cl_2 (50 mL × 2). The combined organic layers were washed twice with water and once with brine, dried over anhydrous magnesium sulfate. After removing the solvent under reduced pressure, the residue was purified by chromatography using hexane/EA (10/1, v/v) as an eluent to yield compound **3a** as an orange solid (130 mg, 66%). ^{1}H NMR (400 MHz, $CDCl_3$) δ: 9.00 (d, J = 2.4 Hz, 1H), 8.46 (dd, J_1 = 9.0 Hz, J_2 = 2.4 Hz, 1H), 8.20 (d, J = 9.0 Hz, 1H), 7.50 (dd, J_1 = 10.6 Hz, J_2 = 8.7 Hz, 4H), 7.30 (t, J = 7.6 Hz, 8H), 7.15 (d, J = 7.8 Hz, 8H), 7.13–7.09 (m, 4H), 7.04 (dd, J = 8.6, 6.8 Hz, 4H). ^{13}C NMR (100 MHz, $CDCl_3$) δ: 155.88, 155.30, 149.50, 149.32, 147.48, 147.04, 146.97, 143.55, 139.73, 131.04, 130.94, 130.77, 130.34, 129.49, 125.43, 125.36, 124.00, 123.91, 122.84, 121.47, 121.29. ESI (*m/z*): Calcd for $C_{44}H_{31}N_5O_2$, 661.25 (M^+); found, 661.24.

3. Results and discussion

The synthesis routes of five D-A-D type monomers **VQ1** ~ **VQ5** and corresponding polymers **PVQ1** ~ **PVQ5** were shown in Scheme 1. Briefly, the preparation of five monomers were achieved in high yields *via* condensation reactions between corresponding benzene-1,2-diamine derivates and a same intermediate diketone **1**, respectively, which was synthesized by Friedel crafts acylation of triphenylamine. The structures of desired V-type monomers were characterized by NMR spectroscopy as well as mass spectrometry (Fig. S1 ~ S12). All these monomers exhibited high thermal stability, with decomposition temperatures around 410 °C at 5% weight loss (Fig. S13), which is higher than most of the triphenylamine derivatives [42,43].

The absorption spectra of five monomers **VQ1** ~ **VQ5** in dichloromethane were shown in Fig. 1a, and the data were summarized in Table 1. All these monomers exhibited two or three distinct absorption bands: the longer wavelength absorption bands around the visible region (400–480 nm) that can be assigned to intramolecular charge transfer (ICT) transitions from the triphenylamine donating groups to the quinoxaline-based accepting moieties, [19]; the shorter and broad wavelength absorption bands in the UV region (300–400 nm) is mainly originated from the π-π* electron transitions of the conjugated molecules. The absorption peak originated from ICT transition of **VQ1** located in 401 nm. It was noted that a linear D-A-D isomer with two triphenylamine group substituted in 5,8-positions of quinoxaline moiety

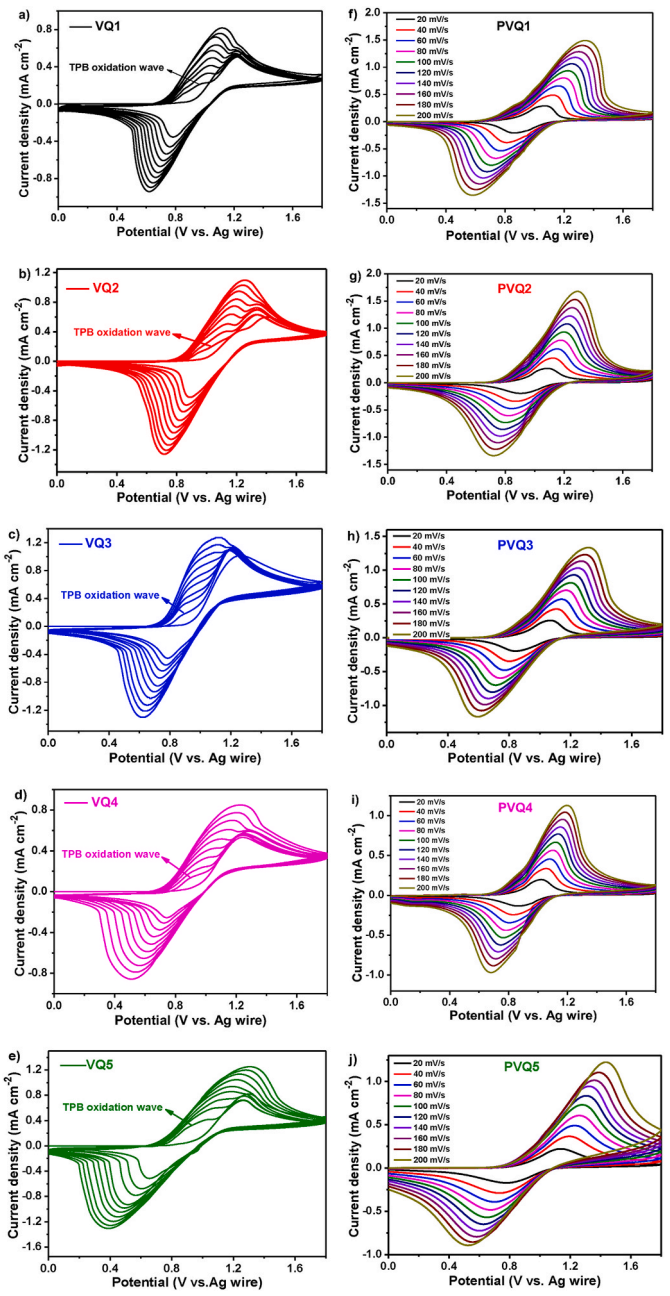

Fig. 3. a~e) CV curves of five monomers in ACN:toluene (1:4, v/v, 2 mM) containing 100 mM $TBAPF_6$ between 0 and 1.8 V for 10 cycles at scan rate of 100 mV s^{-1}, respectively; f~j) CV of **PVQ1** ~ **PVQ5** thin films on ITO in $TPAPF_6$/PC (0.1 M) at scan rate from 20 to 200 mV s^{-1}, respectively.

exhibited a maximum ICT absorption peak around 413 nm reported by Zhou et al. previously [44]. The result implied that a blue-shift was achieved by constructed V-shape D-A-D configuration as compared to that with linear D-A-D type configuration. With the introduction of two methoxy groups on 6- and 7- positions of its quinoxaline moiety, the corresponding ICT absorption peak of **VQ2** exhibited slight hypochromatic shift, probably due to the weakened electron accepting ability of the quinoxaline-based acceptor. In contrast, with the introduction of one or more electron withdrawing groups in quinoxaline moiety, **VQ3**, **VQ4** and **VQ5** exhibited different degrees of redshift in comparison to **VQ1**. As a result, the absorption onset of **VQ5** with additional strong electron-deficient group (-NO_2) extent up to 580 nm.

Cyclic voltammetry (CV) was carried out in CH_2Cl_2 containing 0.1 M tetrabutylammonium hexafluorophosphate ($TBAPF_6$) as a supporting electrolyte to investigate the electrochemical properties of five new D-A-D type monomers **VQ1** ~ **VQ5** (Fig. 1b). As shown in Table 1, these five monomers exhibited similar first oxidation potentials due to the same electron donor parts in them. In order to gain further insight into the configurations of these five monomers and their frontier molecular orbitals, DFT calculations of monomers **VQ1** ~ **VQ5** are carried out at the B3LYP/6-31G** level. As shown in Fig. 2, LUMOs of these V-type monomers are mainly located on the quinoxaline parts, whereas their HOMOs show delocalized electron distributions through the two triphenylamine moieties and their adjacent pyrazine group, respectively. Hence, both orbitals provide overlap between donor and acceptor to guarantee an intramolecular charge transfer transition.

The polymer thin films **PVQ1** ~ **PVQ5** were successfully deposited on ITO/glass *via* electrochemical polymerization of these new monomers (see Fig. 3), which was carried out by a conventional three-electrode system in the solution of monomers in a mixed solvent of methylbenzene/acetonitrile (4/1, v/v), using $TBAPF_6$ as a supporting electrolyte, respectively [45]. As seen in Fig. 3a and 3e, a reversible oxidation peak at 1.2 V was observed for each sample during the first anodic scan, which was attributed to the oxidation of the corresponding triphenylamine moiety [46]. In the second scan an additional shoulder oxidation peak at 1.05 V appeared, which shifted to a higher potential after each successive cycle. The additional peak may be a typical oxidation wave of the tetraphenylbenzidine (TPB) group, suggesting the occurrence of the oxidative coupling between the triphenylamine units (Fig. S14) [47]. In the subsequent voltammetric cycles, the anodic peaks gradually shifted to higher potentials and the cathodic peaks shifted to lower potentials with the increasing intensity of the oxidation peaks. The increase of redox current intensities by successive CV scan implied the formation of the electrochemically active polymeric film on the electrode surface [48]. After ten repeated CV scans between 0 and 1.8 V, an electrochemically deposited thin film was observed on the electrode surface. All five monomers exhibited a similar phenomenon during the electrochemical polymerization process.

Cyclic voltammograms (CVs) of the polymer films **PVQ1** ~ **PVQ5** on ITO was carried out in a three-electrode electrochemical system, in which the polymer films on ITO as working electrode, Pt wire as the counter electrode, Ag wire as the reference electrode, respectively. The cyclic voltammetry (CV) curves of electrodes at different scan rates between 20 and 200 mV s^{-1} were recorded in 0.1 M $TPAPF_6$/PC solutions. As shown in Fig. 3f–3j, a pair of redox peaks of **PVQ1** ~ **PVQ5** electrodes were observed, respectively. The plot of scan rate against the maximum current (*I*) shows the linear relationship (Fig. S15), indicating that the charge transfer process of the redox reaction of these electrode is not limited by the diffusion of counter ions. The result also suggested a good contact between the electro-generated polymeric films and ITO electrode.

Then, we investigated the electrochromic properties of the present polymer **PVQ1** ~ **PVQ5** on ITO electrode by spectroelectrochemistry measurements, which were performed in a bath of 0.1 M $TBAPF_6$/PC. For example, **PVQ1** film in neutral form exhibited a broad absorption band with a peak value around 340 nm corresponding to the overlapping π-π* transition and ICT, of which the intensity decreased gradually under the increasing working potential. Meanwhile, a new absorption peak around 500 nm was observed accompanying the increase of the absorption intensity, which may be attributed from the formation of TPB radical cation [49]. Notably, when a working potential over 1.04 V was applied, the dication of TPB may be formed [50], resulting in a new intense absorption band extend to the near IR region with a peak around 750 nm was appeared, and its intensity reached a maximum value at around 1.2 V (Fig. 4a). As a result, The polymer **PVQ1** exhibited multicolor change from light yellow to orange, and further to blue under certain applied voltage. As shown in Fig. 4b–4f, other four analogues **PVQ2** ~ **PVQ5** exhibited similar electrochromic behaviour.

We further investigated the optical eletrochromism by

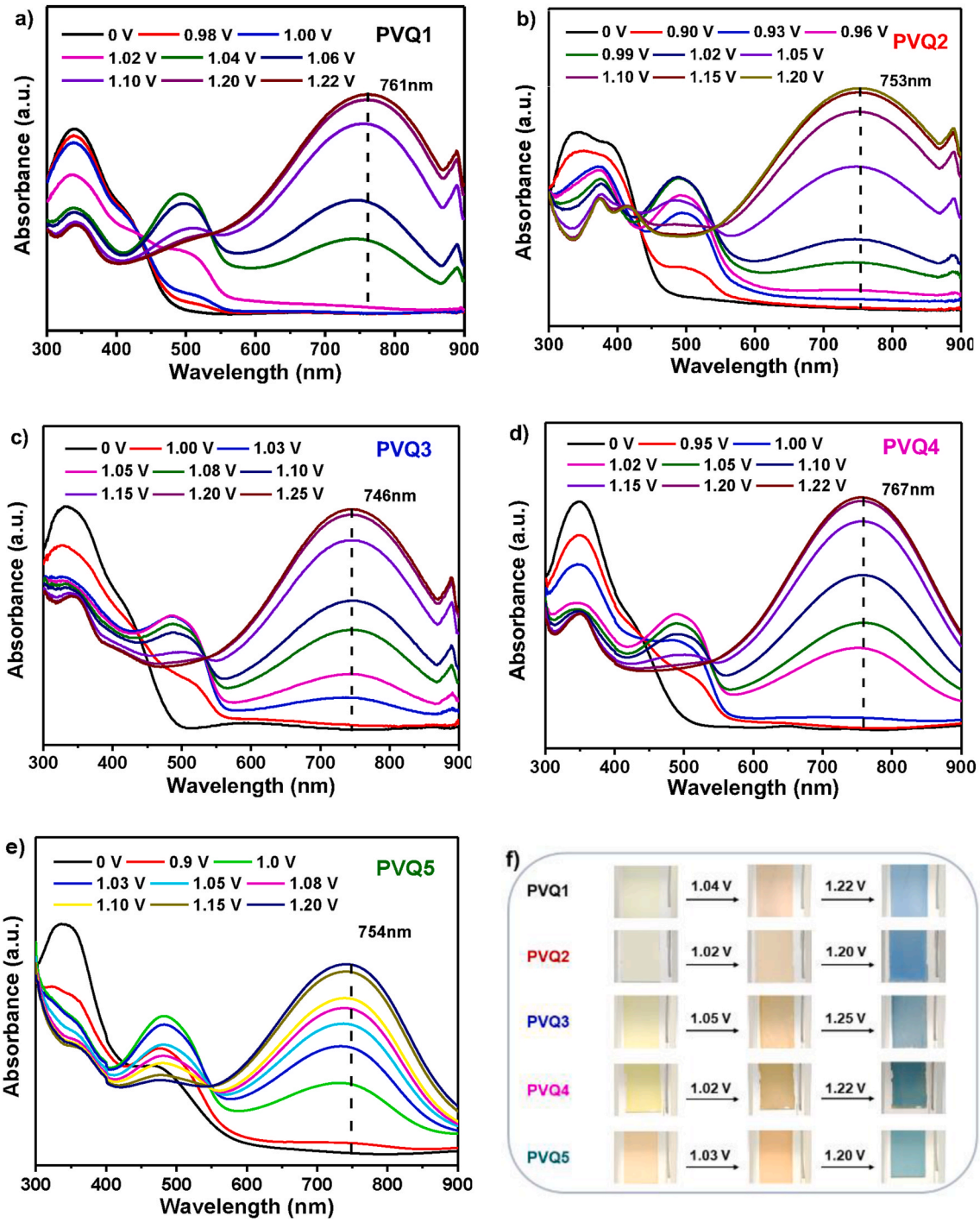

Fig. 4. Electronic absorption spectra of **PVQ1** ~ **PVQ5** thin films on ITO in $TPAPF_6$/PC (0.1 M), respectively.

chronoamperometry with putting on square-wave potential between 0 and the corresponding highest oxidation potentials for **PVQ1** ~ **PVQ5**, respectively (see Fig. 5) [51]. While the films were switched, the transmittance at selected wavelengths was monitored as a function of time with UV–vis–NIR spectroscopy. The response time was calculated at 90% of the full-transmittance change, because it is difficult to perceive any further color change with the naked eye beyond this point [52]. As shown in Fig. 5a and 5e, the optical transmittance of **PVQ1** ~ **PVQ5** film at the longer wavelength peak (around 750 nm) was detected by applying potential between 0 and the corresponding highest oxidation (around 1.2 V) potentials with a residence time of 10 s. As summarized in Table 2, all these five polymers performed high optical contrast over 70% with coloration time (t_c) less than 2 s and bleaching time (t_b) less than 1s. Especially, the t_c and t_b of **PVQ4** was 0.9 s and 0.7 s, which is superior to the reported electrochromic materials based on triphenylamine derivatives [16,28,34,45,46,50]. The faster response time for these five films may be attributed to its D-A-D structure, which might be more favorable for electron transfer within molecules. As shown in Fig. 5f–5j, all these five electrochromic materials exhibited good stability with a little decrease of optical contrast about 5% after 20 cycles switching.

Chrono-absorptometric and chronoamperometric techniques were employed to evaluate the coloration efficiencies of these five novel D-A-D type polymers. The charge/discharge amount (Q_d) was recorded by

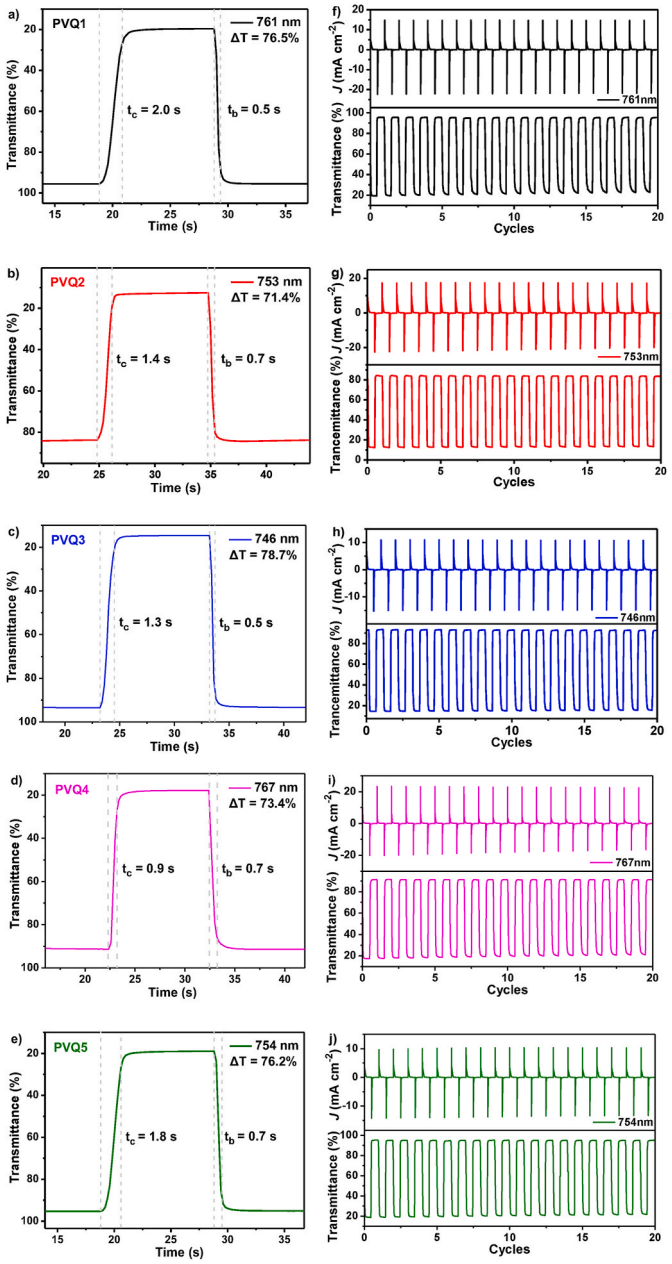

Fig. 5. a~e) Optical contrast and response time of **PVQ1** ~ **PVQ5** thin films around 750 nm, respectively; (f~j) Electrochromic switching stability for **PVQ1** ~ **PVQ5** thin films, respectively.

monitoring the change in current with time (Fig. 5f–5j). Then, we calculated the coloration efficiency (CE) of these five polymers by using the following equations [53].

$$CE = [\log (T_b/T_c)]/Q_d$$

where T_b and T_c are the percent transmittance of bleaching and coloring state at the corresponding wavelength around 750 nm, respectively. As listed in Table 2, CE of these five new electrochromic materials were calculated to be 200 cm^2/C for **PVQ1**, 224 cm^2/C for **PVQ2**, 251 cm^2/C for **PVQ3**, 232 cm^2/C for **PVQ4**, 312 cm^2/C for **PVQ5**, respectively. The electrochromic switch properties around 495 nm of these five polymer were also investigated by the same way, and the results were shown in Fig. S16 and Table S1.

Finally, we fabricated electrochromic devices based on **PVQ1** ~ **PVQ5** films with a sandwich configuration. Briefly, a gel electrolyte containing 0.1 M $TBAPF_6$ in PC solution and 20 wt% poly(methylmethacrylate) (PMMA) was spread on the top of the **PVQ1** ~ **PVQ5** films that were pre-deposited on ITO glass, respectively. Then, a bare ITO glass was covered on the top of electrolyte and sealed by a commercial 3 M tape to prevent leakage [54]. As shown in Fig. 6 and Fig. S17-20, EC devices based on polymers **PVQ1** ~ **PVQ5** exhibited similar electrochromic phenomena with multicolor change from pale yellow to orange, and further to blue upon the increase of applied potentials, respectively. Electrochromic devices based on these five polymers exhibited highest optical contrast over 80% around 750 nm, and exhibited good redox stability after 20 cycles switching, respectively. Moreover, the diversiform color in both bleaching and coloring states of these five electrochromic devices suggested the successful molecular design of the present V-type D-A-D compounds toward tunable electrochromism.

4. Conclusion

In summary, we developed five novel D-A-D type monomers with a common V-shape configuration, in which two triphenylamine groups were introduced into the 2- and 3- position of the quinoxaline derivates. Five polymer films **PVQ1** ~ **PVQ5** were successfully deposited onto the ITO electrodes *via* electro-polymerization, which exhibited large optical contrast, short response time, high coloration efficiency and good redox stability, respectively. Electrochromic devices based on the present D-A-D polymers were also prepared and exhibited efficient electrochromic performance, which further demonstrated the rational structure design of V-shape monomers. Moreover, the multiple and tunable color change among the visible and near IR region guaranteed their potential applications in smart windows.

CRediT authorship contribution statement

Wenyuan Wang: Investigation, Formal analysis, Writing – original draft. **Hongjin Chen:** Synthesis, Formal analysis. **Youfeng Yue:** Formal analysis, Writing – review & editing. **Rui Zhang:** Project administration, Writing – review & editing. **Jian Liu:** Conceptualization, Writing – review & editing, Supervision, Funding acquisition.

Declaration of competing interest

The authors declare that they have no known competing financial interests or personal relationships that could have appeared to influence the work reported in this paper.

Table 2
Optical and electrochromic properties of **PVQ1** ~ **PVQ5** thin films monitored around 750 nm[a].

Polymers	Operation voltage (V)	Transmittance change (ΔT, %)	Bleaching time (t_b, s)	Coloration time (t_c, s)	Charge/discharge amount (Q_d, mC·cm^{-2})	Coloration efficiency (CE, cm^2·C^{-1})
PVQ1	0–1.22 V	76.5	0.5	2.0	2.47/1.76	200
PVQ2	0–1.2 V	71.4	0.7	1.4	2.28/1.51	224
PVQ3	0–1.25 V	78.7	0.5	1.3	2.35/1.24	251
PVQ4	0–1.25 V	73.4	0.7	0.9	2.28/1.51	232
PVQ5	0–1.2 V	76.2	0.7	1.8	2.35/1.24	312

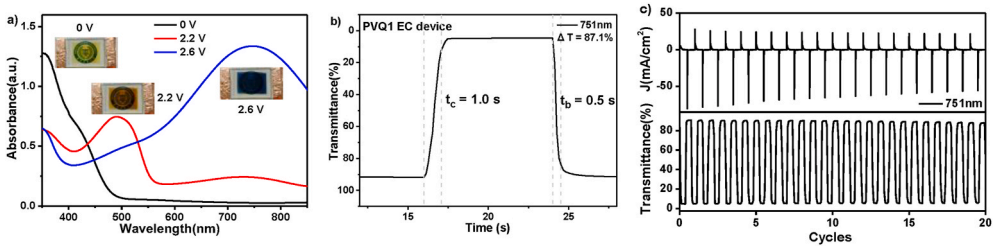

Fig. 6. a) Absorption spectra of a EC device based on **PVQ1** at 0 V, 2.2 V and 2.6 V; b) The transmittance change for the EC device based on **PVQ1** at 751 nm; c) Current consumption and transmittance changes monitored of the EC device based on **PVQ1** at 755 nm during 20 cycles of electrochromic switching between 0 and 2.6 V.

Acknowledgements

This work was supported in part by the Natural Science Foundation of Jiangsu Province (BK20191385), the National Natural Science Foundation of China (21631006), and the High Level Talent Project of Nanjing Forestry University (GXL2018003).

Appendix A. Supplementary data

Supplementary data to this article can be found online at https://doi.org/10.1016/j.dyepig.2021.109615.

References

[1] Yen HJ, Liou GS. Recent advances in triphenylamine-based electrochromic derivatives and polymers. Polym Chem 2018;9(22):3001–18.
[2] Yen HJ, Lin KY, Liou GS. High Tg, ambipolar, and near-infrared electrochromic anthraquinone-based aramids with intervalence charge-transfer behavior. J Polym Sci, Part A: Polym Chem 2012;50(1):61–9.
[3] Zhong Y, Chai Z, Liang Z, Sun P, Xie W, Zhao C, Mai W. Electrochromic asymmetric supercapacitor windows enable direct determination of energy status by the naked eye. ACS Appl Mater Interfaces 2017;9(39):34085–92.
[4] Yen HJ, Lin KY, Liou GS. Transmissive to black electrochromic aramids with high near-infrared and multicolor electrochromism based on electroactive tetraphenylbenzidine units. J Mater Chem 2011;21(17):6230–7.
[5] Chuang YW, Yen HJ, Wu JH, Liou GS. Colorless triphenylamine-based aliphatic thermoset epoxy for multicolored and near-infrared electrochromic applications. ACS Appl Mater Interfaces 2014;6(5):3594–9.
[6] Bingöl B, Camurlu P, Toppare L. Synthesis and characterization of poly(thiophen-3-yl acetic acid 4-pyrrol-1-yl phenyl ester-co-N-methylpyrrole) and its application in an electrochromic device. J Appl Polym Sci 2006;100(3):1988–94.
[7] Liou GS, Chang CW. Highly stable Anodic electrochromic aromatic polyamides ContainingN,N,N‘,N‘-Tetraphenyl-p-Phenylenediamine moieties: synthesis, electrochemical, and electrochromic properties. Macromolecules 2008;41(5):1667–74.
[8] Chen CJ, Yen HJ, Chen WC, Liou GS. Novel high-performance polymer memory devices containing (OMe)2tetraphenyl-p-phenylenediamine moieties. J Polym Sci, Part A: Polym Chem 2011;49(17):3709–18.
[9] Xing J, Yue Y, Zhang R, Liu J. Molecular engineering of head-tail terpyridine-Fe(II) coordination polymers employing alkyl chain linkers toward enhanced electrochromic performance. Dyes Pigments 2021;189:109233.
[10] Xing Z, Wang Y, Han Y, Zhai Y, Tian Y, Qi S, Zhu X, Jiang Z, Chen Z. The effect of constructing discontinuous side chain D-A structure on high-performance poly (ether sulfone)s optoelectronic materials. Dyes Pigments 2021;189:109259.
[11] Yu T, Han Y, Yao H, Chen Z, Guan S. Polymeric optoelectronic materials with low-voltage colorless-to-black electrochromic and AIE-activity electrofluorochromic dual-switching properties. Dyes Pigments 2020;181:108499.
[12] Zeng Z, Wu J, Chen Q, Shi Y, Zheng J, Xu C. A multifunctional triphenylamine schiff-base compound with novel self-assembly morphology transitions. Dyes Pigments 2019;170:107649.
[13] Zhang L, Xu G, Wang L, Wang B, Ren Z, Dou S, Song S, Pan M, Li X, Li Y. Achieving variable infrared emissivity modulation regions of poly(aniline) films:the effect of film surface morphology on the optical tunability. Dyes Pigments 2021;187:109084.
[14] Wang J, Liu J, Hu M, Zeng J, Mu Y, Guo Y, Yu J, Ma X, Qiu Y, Huang Y. A flexible, electrochromic, rechargeable Zn//PPy battery with a short circuit chromatic warning function. J Mater Chem 2018;6(24):11113–8.
[15] Chen Y, Yin Y, Xing X, Fang D, Zhao Y, Zhu Y, Ali MU, Shi Y, Bai J, Wu P, Shen CKF, Meng H. The effect of Oligo(ethylene oxide) side chains: a strategy to improve contrast and switching speed in electrochromic polymers. ChemPhysChem 2020;21(4):321–7.
[16] Sun N, Su K, Zhou Z, Tian X, Wang D, Vilbrandt N, Fery A, Lissel F, Zhao X, Chen C. Synergistic effect between electroactive tetraphenyl-p-phenylenediamine and AIE-active tetraphenylethylene for highly integrated electrochromic/electrofluorochromic performances. J Mater Chem C 2019;7(30):9308–15.
[17] Dai Y, Li W, Chen Z, Zhu X, Liu J, Zhao R, Wright DS, Noori A, Mousavi MF, Zhang C. An air-stable electrochromic conjugated microporous polymer as an emerging electrode material for hybrid energy storage systems. J Mater Chem 2019;7(27):16397–405.
[18] Bagdžiūnas G, Palinauskas D, Ramanavičius A. Towards colourless-to-green electrochromic smart glass based on a redox active polymeric semiconductor containing carbazole moiety. Dyes Pigments 2020;177:108328.
[19] Çakal D, Akdag A, Cihaner A, Önal AM. Effect of the donor units on the properties of fluorinated acceptor based systems. Dyes Pigments 2021;185:108955.
[20] Capodilupo A-L, Manni F, Corrente GA, Accorsi G, Fabiano E, Cardone A, Giannuzzi R, Beneduci A, Gigli G. Arylamino-fluorene derivatives: Optically induced electron transfer investigation, redox-controlled modulation of absorption and fluorescence. Dyes Pigments 2020;177:108325.
[21] Chen C, Yan Q. Achieving excellent colorimetric properties of low-cost black to transmissive switching electrochromic polymers by incorporating of spacing units into copolymers of 3,4-propylenedioxythiophene and benzothiadiazole. Dyes Pigments 2020;178:108378.
[22] Gu H, Xue Y, Hu F, Jian N, Lin K, Wu T, Liu X, Xu J, Lu B. Design of twisted conjugated molecular systems towards stable multi-colored electrochromic polymers. Dyes Pigments 2020;183:108648.
[23] Cai G, Cui P, Shi W, Morris S, Shi NL, Chen J, Ciou JH, Paidi VK, Lee KS, Li S, Lee PS. One-dimensional π-conjugated coordination polymer for electrochromic energy storage device with exceptionally high performance. Adv Sci 2020;7(20):1903109.
[24] Cai G, Chen J, Xiong J, Lee-Sie Eh A, Wang J, Higuchi M, Lee PS. Molecular level assembly for high-performance flexible electrochromic energy-storage devices. ACS Energy Lett 2020;5(4):1159–66.
[25] Atighilorestani M, Jiang H, Kaminska B. Electrochromic-polymer-based switchable plasmonic color devices using surface-relief nanostructure pixels. Adv Opt Mater 2018;6(23):1801179.
[26] Huang C-L, Kung Y-R, Shao Y-J, Liou G-S. Synthesis and characteristics of novel TPA-containing electrochromic poly(ether sulfone)s with dimethylamino substituents. Electrochim Acta 2021;368:137552.
[27] Huang Z, Mou H, Xie J, Li F, Gong C, Tang Q, Fu XK. AIE-active electrochromic materials based on tetraphenylethylene cored benzoates with high optical contrast and coloration efficiency. Sol Energy Mater Sol Cells 2020;206:110293.
[28] Liu Y, Liu T, Pang L, Guo J, Wang J, Qi D, Li W, Shen K. Novel triphenylamine polyamides bearing carbazole and aniline substituents for multi-colored electrochromic applications. Dyes Pigments 2020;173:107995.
[29] Rybakiewicz R, Ganczarczyk R, Charyton M, Skorka L, Ledwon P, Nowakowski R, Zagorska M, Pron A. Low band gap donor-acceptor-donor compounds containing carbazole and naphthalene diimide units: synthesis, electropolymerization and spectroelectrochemical behaviour. Electrochim Acta 2020;358:136922.
[30] Chen W-H, Li F-W, Liou G-S. Novel stretchable ambipolar electrochromic devices based on highly transparent AgNW/PDMS hybrid electrodes. Adv Opt Mater 2019;7(19):1900632.
[31] de Araujo MH, Silva WM, Rocco MLM, Donnici CL, Calado HDR. Preparation and characterization of a quaternary acceptor-donor-acceptor-donor (A-D-A-D) nanohybrid material for electrochromic device application. Electrochim Acta 2020;350:136212.
[32] Higginbotham HF, Czichy M, Sharma BK, Shaikh AM, Kamble RM, Data P. Electrochemically synthesised xanthone-cored conjugated polymers as materials for electrochromic windows. Electrochim Acta 2018;273:264–72.
[33] Cimrová V, Výprachtický D, Pokorná V, Babičová P. Donor-acceptor copolymers with 1,7-regioisomers of N,N'-dialkylperylene-3,4,9,10-tetracarboxydiimide as materials for photonics. J Mater Chem C 2019;7(46):14678–92.
[34] Constantin CP, Bejan AE, Damaceanu MD. Synergetic effect between structural manipulation and physical properties toward perspective electrochromic n-type polyimides. Macromolecules 2019;52(21):8040–55.
[35] Lv XJ, Xu LB, Qian L, Yang YY, Xu ZY, Li J, Zhang C. A conjugated copolymer bearing imidazolium-based ionic liquid: electrochemical synthesis and electrochromic properties. Chin J Polym Sci 2020:1–8.
[36] Huang X, Niu Q, Fan S, Zhang Y. Highly oriented lamellar polyaniline with short-range disorder for enhanced electrochromic performance. Chem Eng J 2020:128126.

[37] Li D, Yang Y, Yang C, Zhang W, Wang Y, Lin X, Gao Y, Lv X, Niu H, Wang W. Aggregation-induced emission enhancement-active triarylamine-based polyamides containing fused ring groups towards electrochromic smart window and sensor for HCl and TNP. Dyes Pigments 2021;184:108799.
[38] Lin X, Li N, Zhang W, Huang Z, Tang Q, Gong C, Fu X. Synthesis and electrochromic properties of benzonitriles with various chemical structures. Dyes Pigments 2019; 171:107783.
[39] Liu Y, Liu F, Wang J, Huang H, Yan S, Gao S, Wang L, Huang W, Qin T. Tetrakis (N-phenothiazine) spirobifluorene-based hole-transporting material towards high photovoltage perovskite photovoltaics for driving electrochromic devices. Dyes Pigments 2021;188:109164.
[40] Zhang W, Niu H, Yang C, Wang Y, Lu Q, Zhang X, Niu H, Zhao P, Wang W. Electrochromic and electrofluorochromic bifunctional materials for dual-mode devices based on ladder-like polysilsesquioxanes containing triarylamine. Dyes Pigments 2020;175:108160.
[41] Zhang Y, Shi X, Xiao S, Xiao D. Visible and infrared electrochromism of bis(2-(2-(2-hydroxyethoxy)ethoxy)ethyl) viologen with sodium carboxymethyl chitosan-based hydrogel electrolytes. Dyes Pigments 2021;185:108893.
[42] Chen Y, Ling Y, Ding L, Xiang C, Zhou G. Quinoxaline-based cross-conjugated luminophores: charge transfer, piezofluorochromic, and sensing properties. J Mater Chem C 2016;4(36):8496–505.
[43] Yue Y, Kang J, Yu M. The synthesis and photophysical properties of novel triphenylaminederivatives containinga,b-diarylacrylonitrile. Dyes Pigments 2009; 83:72–80.
[44] Lu X, Fan S, Wu J, Jia X, Wang Z, Zhou G. Controlling the charge transfer in D−A−D chromophores based on pyrazine derivatives. J Org Chem 2014;79: 6480–9.
[45] Ma F, Liu F, Hou Y, Niu H, Wang C. Electrochromic materials based on novel polymers containing triphenylamine units and benzo[c][1,2,5]thiadiazole units. Synthetic Met 2020;259:116235.
[46] Hsiao S-H, Huang Y-P. Redox-active and fluorescent pyrene-based triarylamine dyes and their derived electrochromic polymers. Dyes Pigments 2018;158:368–81.
[47] Lu Q, Yang C, Qiao X, Zhang X, Cai W, Chen Y, et al. Multifunctional AIE-active polymers containing TPA-TPE moiety for electrochromic, electrofluorochromic and photodetector. Dyes Pigments 2019;166:340–9.
[48] Zeng J, Li H, Wan Z, Ai L, Liu P, Deng W. Colorless-to-black electrochromic materials and solid-state devices with high optical contrast based on cross-linked Poly(4-vinyltriphenylamine). Sol Energy Mater Sol Cells 2019;195:89–98.
[49] Hao Q, Li ZJ, Lu C, Sun B, Zhong YW, Wan LJ, Wang D. Oriented two-dimensional covalent organic framework films for near-infrared electrochromic application. J Am Chem Soc 2019;141(50):19831–8.
[50] Hsiao S-H, Liao W-K, Liou G-S. A comparative study of redox-active, ambipolar electrochromic triphenylamine-based polyimides prepared by electrochemical polymerization and conventional polycondensation methods. Polym Chem 2018;9 (2):236–48.
[51] Zhang Q, Tsai CY, Li LJ, Liaw DJ. Colorless-to-colorful switching electrochromic polyimides with very high contrast ratio. Nat Commun 2019;10(1):1–8.
[52] Lin HT, Huang CL, Liou GS. Design, synthesis, and electrofluorochromism of new triphenylamine derivatives with AIE-active pendent groups. ACS Appl Mater Interfaces 2019;11(12):11684–90.
[53] Ding G, Zhou H, Xu J, Lu X. Electrofluorochromic detection of cyanide anions using a benzothiadiazole-containing conjugated copolymer. Chem Commun 2014;50(6): 655–7.
[54] Pietsch M, Rödlmeier T, Schlisske S, Zimmermann J, Romero-Nieto C, Hernandez-Sosa G. Inkjet-printed polymer-based electrochromic and electrofluorochromic dual-mode displays. J Mater Chem C 2019;7(23):7121–7.